Chemistry–A European Journal

Supporting Information

Continuous isomerisation of 2,5-dimethylfuran to 2,4-dimethylfuran over Ga-silicate

Christopher Sauer, Guido J. L. de Reijer,* Barbara Wilfinger, Anders Hellman, and Per-Anders Carlsson*

Supplementary Information
Continuous isomerisation of 2,5-dimethylfuran to 2,4-dimethylfuran over Ga-silicate

Christopher Sauer[a], Guido J.L. de Reijer[a,*], Barbara Wilfinger[b], Anders Hellman[b], Per-Anders Carlsson[a,*]

[a]Department of Chemistry and Chemical Engineering,
Chalmers University of Technology,
SE-41296 Göteborg, Sweden

[b]Department of Physics,
Chalmers University of Technology,
SE-41296 Göteborg, Sweden

Supplementary Information

Table of contents

1. Catalysts and materials characterisation

Physico-chemical properties of the catalysts are summarised in table S1, including references to additional information in the literature. The catalysts used in this study are commercial products (H-ZSM-5, AkzoNobel), or were prepared by hydrothermal synthesis (Silicalite-1 and Ga-silicate, 5 days at 170 °C) as described elsewhere [1, 2]. In short, a sol-gel was prepared by hydrolysis of tetraethyl orthosilicate in water and oxalic acid (pH 2), followed by mixing with gallium nitrate hydrate and 1.0 M tetrapropylammonium hydroxide. Addition of 1 M NaOH solution raised the gel to pH 11 before hydrothermal synthesis. For the synthesis of Silicalite-1, gallium nitrate hydrate was not added to the mixture. After crystallisation, the samples were washed, filtered and freeze-dried overnight after which the template was burned off at 500 °C for 5 h (5 °C/min) in air. For Ga-silicate, ion exchange was performed twice in 1 M ammonium nitrate solution followed by washing, filtration, and freeze-drying. A final calcination step at 500 °C for 1 h (10 °C/min) resulted in the H^+-form of the zeotype.

Table S1: Physico-chemical properties of the catalysts. Further characterisation of the materials is available. M = Al or Ga.

Sample	SiO_2/M_2O_3	SA $\frac{m^2}{g}$	SA_{micro} $\frac{m^2}{g}$	SA_{ext} $\frac{m^2}{g}$	V_{micro} $\frac{cm^3}{g}$	Acid site density[a] before $\frac{mmol}{g}$	spent	Ref. info.
H-ZSM-5(22)	22	412	386	26	0.158	0.560	0.351	[2, 3]
Silicalite-1	-	395	386	9	0.175	0.002	0.002	[2, 4, 5]
Ga-Silicate	67	365	338	27	0.145	0.102	0.011	[1, 2, 5]

[a] Acid site density determined by NH_3-TPD of the catalyst before the reaction (after pretreatment) and after the reaction (spent catalyst, before oxidative regeneration) consisting of 10 hours 2,5-dmf conversion at 450 °C. See also figure S3.

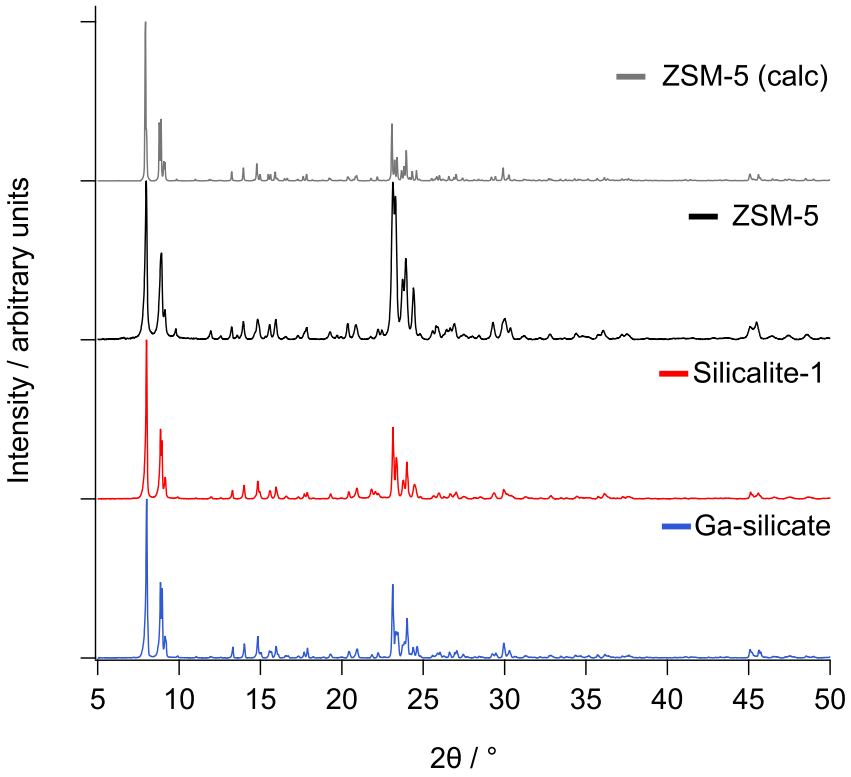

Figure S1: X-ray diffractogram patterns of the tested materials including a calculated pattern of ZSM-5 using crystal data and Pseudo-Voigt for the peak shape. [6, 7]

After synthesis, the presence of the MFI framework was determined with powder X-ray diffraction (XRD) on a Bruker AXS D8 Discover diffractometer (Cu-Kα, 0.15406 nm) and the resulting diffractograms are shown in figure S1. The catalysts' textural properties were determined by N_2-physisorption at 77 K on a Micromeritics Tristar 3000 instrument after drying the materials under N_2-flow for 16 h at 250 °C. The isotherms are shown in figure S2. Elemental analyses of the catalyst powders were carried out by X-ray fluorescence (XRF) using a PANalytical AXIOS instrument and are shown in table S2. The corresponding Si/Al was 11 for the H-ZSM-5 sample and the Si/Ga ratio was found to be 33 for Ga-silicate.

Analysis of the catalyst morphologies is described by electron microscopy elsewhere [1, 2, 3, 8, 5]. Briefly, Silicalite-1 crystals are coffin-shaped while ZSM-5(11) contains both coffin-shaped and cubic-shaped crystals [2, 3]. Ga-silicate crystals are cubic-shaped and include larger, connected intergrown crystals, suggesting the presence of mesopores [1]. For all samples, irregular structures were identified on the external facets, suggesting the

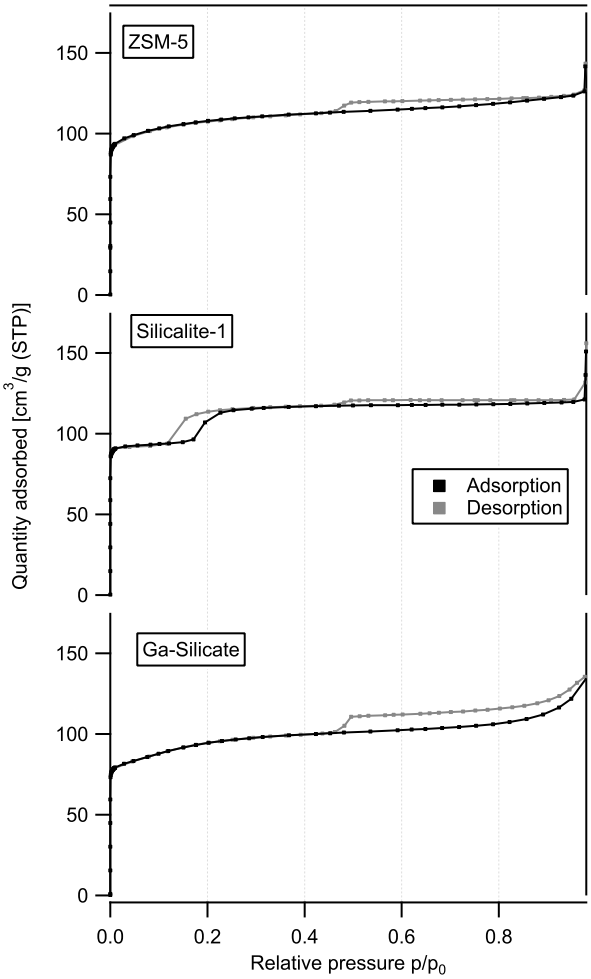

Figure S2: N_2-sorption isotherms at 77K of the catalyst samples. Samples were pretreated at 250 °C for 16 h under N_2 flow.

Table S2: Chemical analyses by XRF. M = Al, Ga.

sample	SiO_2/M_2O_3	Al	Ga	Na	S	K	Ti	Fe	Zr	Ca
		wt%				/wt%				
H-ZSM-5	22	3.49	0	0	0.011	0	0.020	0.058	0.007	0
Silicalite-1	-	0	0	0.313	0	0.101	0	0	0	0
Ga-Silicate	67	0.043	3.23	0	0	0	0	0	0	0.013

presence of impurities or the potential migration of some Al or Ga species during calcination [1].

The presence of Ga inside the MFI framework was observed in another work by *in situ* infrared spectroscopy in diffuse reflectance mode (DRIFTS) based on the vibration at 3616 cm^{-1} which confirms Brønsted acid sites caused by the OH stretch vibration in the -Ga-O(H)-Si- species. In comparison, the -Al-O(H)-Si vibration in Al-silicate (ZSM-5) is observed at 3610 cm^{-1} and thus this shift to higher wavenumbers indicates weaker Brønsted acid strength of the Ga-silicate sample [4, 5].

2. Chemical flow reactor and on-line analysis for catalytic tests

Catalytic measurements and determination of acidity were carried out in a chemical flow reactor. The reactor consists of a quartz glass tube (ID = 4 mm) surrounded by a metal coil and insulation for resistive heating. The catalyst samples (ca. 65 mg) were pressed into pellets (5 bar), ground, and sieved to grains of 300 µm to 350 µm particle size to avoid detrimental pressure drop. These grains were held in place by plugs made of quartz wool (Sigma Aldrich). The catalyst temperature was measured by a K-type thermocouple that was inserted in the catalyst bed. Another thermocouple was placed in front of the catalyst and used to control the inlet gas temperature with a PID regulator (Eurotherm, Worthing, UK). Mass flow controllers (Bronkhorst Hi-Tech, Low-ΔP-flow) were used to introduce feed gas mixtures of O_2 (100%), NH_3 (4% in Ar) and Ar (100%). The liquid reactant 2,5-dmf (liquid, Apollo scientific 99% or Sigma-Aldrich $\geq$ 99%) was introduced via a gas saturator with argon as a carrier gas to obtain reactant concentrations between 300 and 1050 ppm. The total flow in the reactor was 150, 300 or 400 mL_n/min.

The analytical instrumentation, consisting of an ion-molecule-reaction mass spectrometer (IMR-MS, Airsense Compact, V&F) and an FTIR gas analyzer (MKS MultiGas 2030) was directly connected via heated Swagelok connections to the reactor outlet. Monitoring of the gas composition and quantification of reaction products were done according to a previously described method combining mass spectrometry and FTIR spectroscopy [8]. To quantify ammonia in the gas stream, some adjustments and additions to the analysis bands were required. Details of the analysis conditions (IR-bands, m/z values) are shown in table S3. IR spectra were recorded every 7.5 s or 15 s between 4000 cm^{-1} to 600 cm^{-1} with a resolution of 0.5 cm^{-1}. The MKS software suite MG2000 v.10.2. and FTIR-library v.R3 supplemented with in-house calibrations described elsewhere [8] were used for spectra collection and analysis. At the beginning of each experiment, a background spectrum in Ar was taken where the IR cell temperature was 191 °C.

To remove coke depositions and/or adsorbed species before each experiment, the catalyst was pretreated in 20% O_2 during a temperature ramp of 20 °C min^{-1} from room temperature up to ca. 600 °C at which it was dwelled for at least 30 min. Catalytic tests were performed as step response experiments, in which the catalyst was continuously exposed to reactant 2,5-dmf for e.g. 2 h, 10 h and 48 h at a steady temperature, e.g. 350 °C

Table S3: Information about the analysed molecules of the gas stream. Xe = 12.13 eV (for CO (28), CO_2 (44), O_2 (33), Ar (40)) or Hg = 10.44 eV (all others) as ionisers. Based on a previously described analysis method with additions and adaptions[8].

Compound	Formula	m/z	IR band /cm^{-1}
Other rings			
2-methylnaphthalene	$C_{11}H_{10}$	142	785.38 – 831.18
Naphthalene	$C_{10}H_8$	128	758.62 – 807.32
Indene	C_9H_8	116	2811.26 – 3176.23
2-methyl-CPO	C_6H_8O	(96), 68	1668.88 – 1809.90
3-methyl-CPO	C_6H_8O	(96), 68	1701.42 – 1811.83
Furans			
2,5-dimethylfuran	C_6H_8O	96, (81)	1168.43 – 1282.69
2,4-dimethylfuran	C_6H_8O	(96), 68	1074.17 – 1174.70
2-methylfuran	C_5H_6O	(81)	1117.57 – 1176.87
BTX			
Benzene	C_6H_6	78	606.51 – 726.80
Toluene	C_7H_8	92	689.44 – 769.95
o-xylene	C_8H_{10}	106	702.45 – 779.59
p-xylene	C_8H_{10}	106	735.32 – 867.92
Olefins			
Ethene	C_2H_4	(28), 27	900.12 – 1000.16
Propene	C_3H_6	42, (41)	900.61 – 1019.69
1,3-butadiene	C_4H_6	(54), 39	822.26 – 977.02
C1			
Methane	CH_4	-	3000.25 – 3176.23
Carbon monoxide	CO	28	2146.16 – 2159.90
Carbon dioxide	CO_2	44	2223.57 – 2280.94
Formaldehyde	CH_2O	(30)	2698.93 – 2822.36
Water	H_2O	18	1416.97 – 1502.31
Ammonia	NH_3	16	903.98 – 977.27

and 450 °C. The 10-hour-long experiments included a stepwise increase of reactant concentration just after 10 h TOS to observe the response of product concentrations.

3. Ammonia-TPD

In the above-described reactor, temperature programmed desorption (TPD) measurements of NH_3 were carried out to determine the total amount of acid sites of the catalysts assuming that one acid site adsorbs one ammonia molecule [9]. The catalyst samples were exposed to two 60 min pulses of 200 ppm NH_3 to ensure complete saturation of the catalysts by NH_3 at 150 °C. Then the samples were purged with pure Ar for 60 min followed by a temperature ramp of 10 °C min^{-1} from 150 °C to 550 °C to desorb NH_3. The TPD profile is analysed by applying a baseline correction and deconvolution using symmetric Gaussian functions. In this way, the number of acid sites before the 10 h long catalytic tests and after the 10 h long catalytic tests (without oxidative regeneration of the catalyst; spent catalyst) is determined. These NH_3-TPD measurements for ZSM-5 and Ga-silicate catalysts are shown in figure S3. The acid site densities are summarised in table S1.

The experimentally estimated TOF is derived from the conversion of 2,5-dmf into 2,4-dmf at different TOS (10 h conversion at 450 °C), as well as the number of acid sites determined by NH_3-TPD. The following assumptions have been made: each acid site binds to one NH_3 molecule, each acid site is accessible to 2,5-dmf, and a quasi-steady state is assumed in which the produced coke species are disregarded.

4. Carbon mass balance and selectivity

The carbon mass balance is based on the inlet feed of 2,5-dmf. The carbon balance describes the difference between the inlet feed of the reactant and the sum of all detected product species during a catalytic conversion plus the amount of carbon that was deposited as coke on the catalyst surface and was later detected as CO and CO_2. The carbon mass balance was usually greater than 90%, which means that less than 10% of products were not identified. Some carbon is stored on the zeolite as coke and can thus only be quantified during an oxidative regeneration treatment of the catalyst after the catalytic experiment. Because of this, the shown selectivities do not take into consideration the amount of coke formed during catalytic reactions. During the catalytic experiment of 10 hours at 450 °C, the amount of coke deposited on the catalysts was found to be 3.4 and 4.9 % of the total formed products for Ga-silicate and H-ZSM-5, respectively. This means that if the coke is taken into account for selectivity calculations, the given selectivities will be slightly lower.

The carbon mass balance consists of the concentrations of all product species detected according to the method described above (see also table S3) and formed in relevant concentrations C (typically $\geq$1 %). These products include the following species: 2,4-dimethylfuran (2,4-dmf), methylfuran, 2-methyl-2-cyclopentenone (2-mcpo), 3-methyl-2-cyclopentenone (3-mcpo), benzene, toluene, indene, ethene, propene, butadiene, methane, CO and CO_2. To calculate the conversion, the product concentrations are normalised to

account for the reaction stoichiometry by multiplication with their number of carbon atoms n, followed by division by the number of carbon atoms in the reactant 2,5-dmf (6 carbon atoms). The conversion X can then be calculated as follows:

$$X = 1 - \frac{C_{\text{2,5-dmf}}}{\sum \frac{n}{6} \cdot C_{\text{all products}} + C_{\text{2,5-dmf}}} \tag{1}$$

Similarly, the selectivity S of each species can be calculated as follows:

$$S = \frac{n \cdot C_{\text{product}}}{6 \sum \frac{n}{6} \cdot C_{\text{all products}}} \tag{2}$$

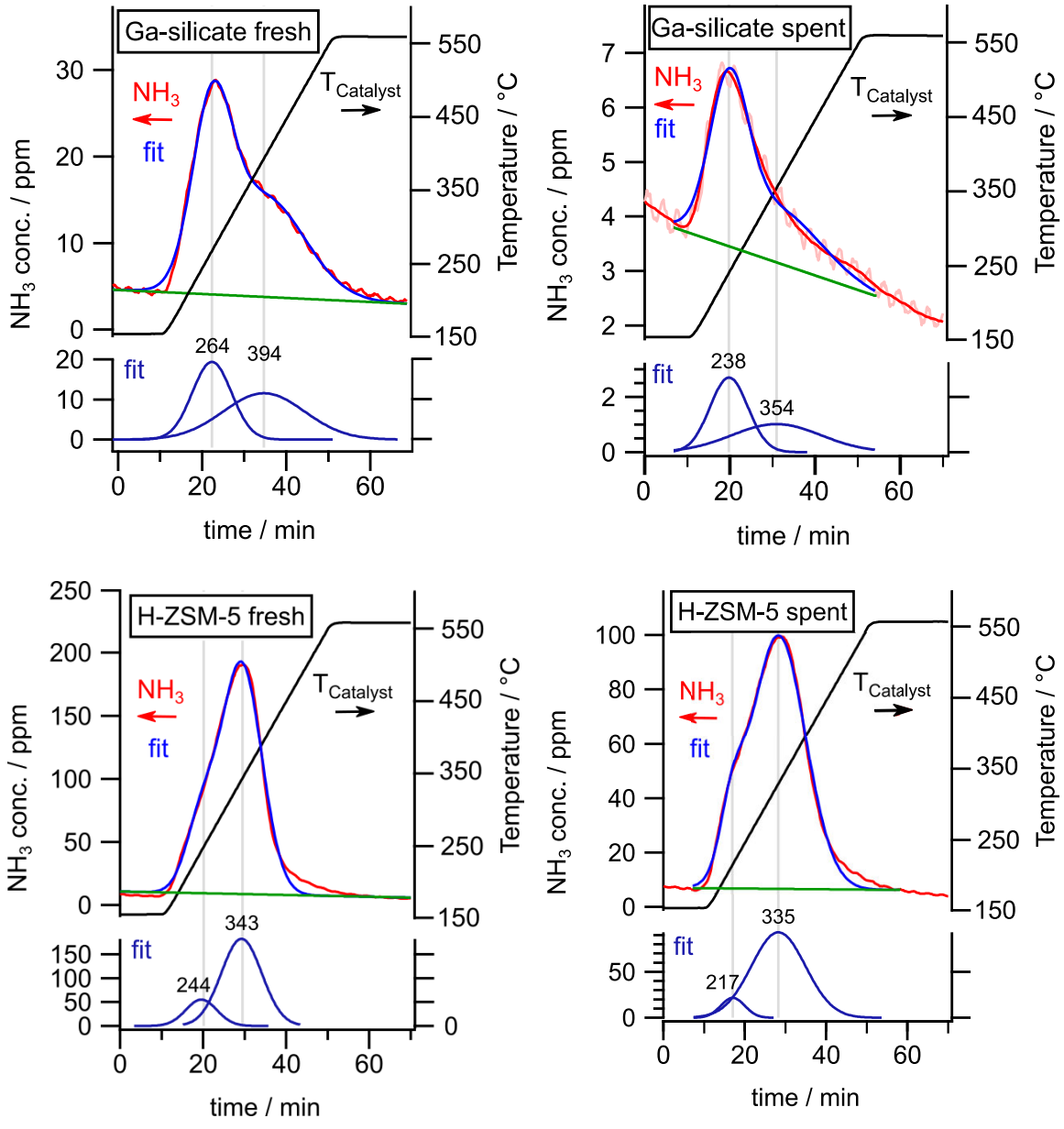

Figure S3: NH_3-TPD profiles of catalysts H-ZSM-5 and Ga-silicate directly before (fresh) and after (spent) the 10 h 2,5-dmf conversion experiment. After NH_3 saturation and 90 min purging with pure Ar at 150 °C, the temperature of the catalyst (black, right axes) is increased to 550 °C with a ramp of 10 °C/min. Desorbed ammonia (red, left axes) is fitted (light blue) after baseline (green) subtraction with symmetric Gaussian functions (blue, lower panels). The desorption temperatures are noted above the fitted peaks. Total flow 300 mL_N/min

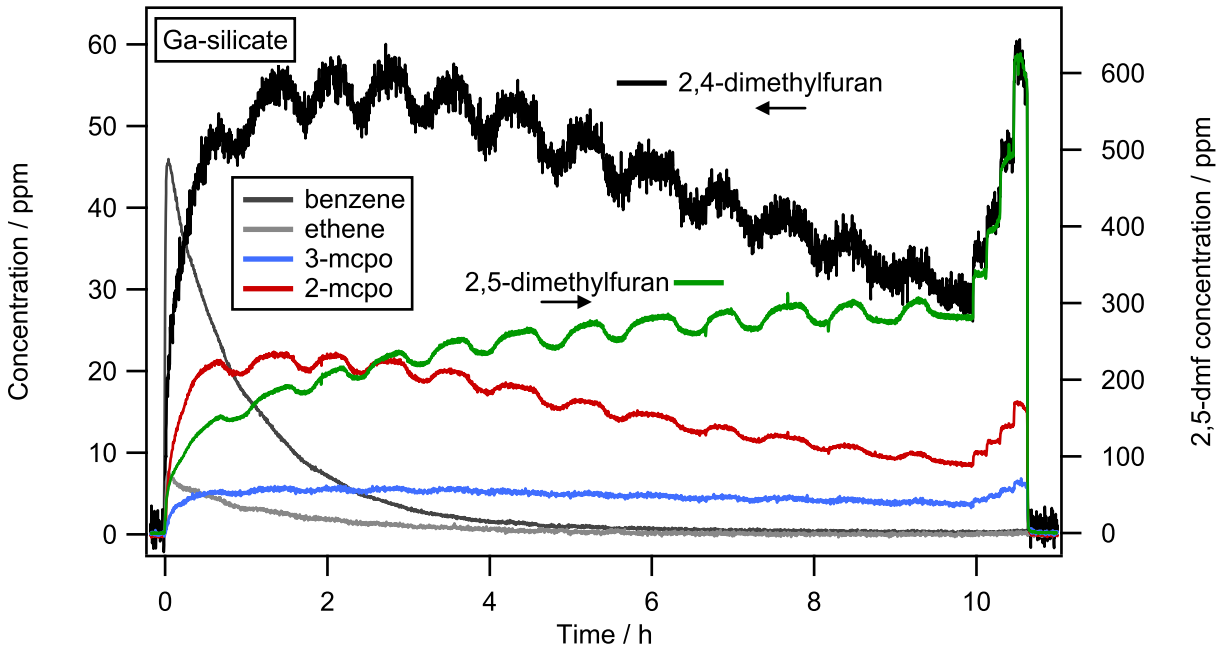

Figure S4: Concentration profiles of the reactant (right axis) and products (left axis) benzene, 2,4-dmf, ethene, 3-mcpo and 2-mcpo during catalytic conversion of 2,5-dimethylfuran over 68.8 mg Ga-Silicate at 450 °C. After 10 h TOS, the 2,5-dmf feed was increased stepwise from 400 ppm to approx. 800 ppm.

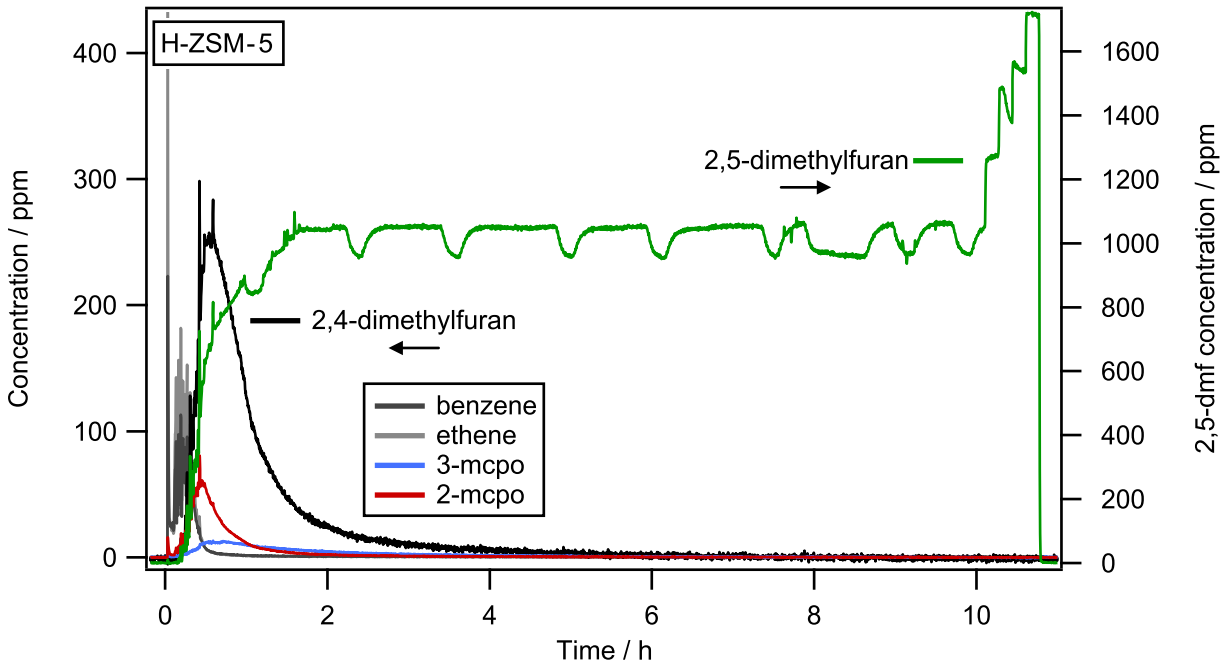

Figure S5: Concentration profiles of the reactant (right axis) and products (left axis) benzene, 2,4-dmf, ethene, 3-mcpo and 2-mcpo during catalytic conversion of 2,5-dimethylfuran over 65.6 mg H-ZSM-5 at 450 °C. After 10 h TOS, the 2,5-dmf feed was increased stepwise from 1100 ppm to approx. 1700 ppm.

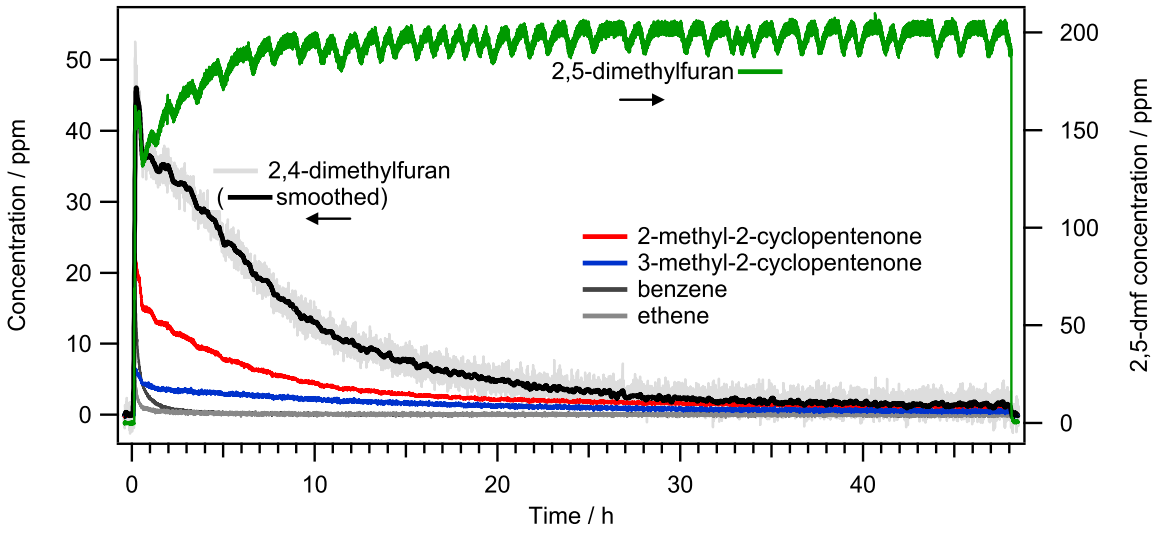

Figure S6: Concentration profiles of the reactant (right axis) and selected aromatic, olefinic and isomer products (left axis) during a 48 h lasting catalytic conversion experiment over 68.8 mg Ga-Silicate (used after the 10 h experiment as in figure 1 in main article and figure S4 450 °C. Total flow 400 mL_N/min, Ar as balance, feed: 200 ppm 2,5-dimethylfuran.

5. Density functional theory calculations

The calculations were performed using GPAW [10, 11]. The projector augmented wave method [12] was used to model the interaction between the valence electrons and the core. The Kohn–Sham orbitals and the corresponding density were represented using plane-waves with an energy cutoff of 600 eV. The Brillouin zone was sampled using the Γ-point approximation. Reciprocal space integration over the Brillouin zone was approximated with Fermi–Dirac distribution with a width of 0.1 eV. The exchange-correlation interaction was treated using the vdW-DF-cx functional, [13, 14] which includes van der Waals interactions in the exchange-correlation.

The lattice parameters of the MFI structure are calculated to be 20.08, 19.98, 13.43 Å, which agree well with experimental values. The Ga atom was put at the crossing between the straight and sinusoidal channels in the ZSM-5 framework. The gas-phase molecules were treated in a cubic box with sides of 10 Å.

Geometries were relaxed until the maximum force was less than 0.03 eV/Å. The vibrational analysis used central differences to obtain the Hessian matrix with a displacement of 0.01 Å. The transition states (TS) were obtained using the climbing NEB method, as implemented in ASE [15].

The relative stability of the reaction intermediate states was compared by calculating the change in Gibbs free energy:

$$\Delta G\left(T, \Delta\mu\right) = \Delta H - T \cdot \Delta S(T) - \Delta\mu. \tag{3}$$

T is temperature, and $\Delta\mu$ is the change in chemical potential between 0 K and the condition of interest. Here, $\Delta\mu = \Delta\mu_{2,5-\mathrm{dmf}}$.

The translational entropy of 2,5-dmf and 2,4-dmf were calculated using the ideal gas approximation, whereas all vibrations were calculated using the harmonic approximation. Rotations were treated by the rigid motor model. The entropy of gas-phase molecules in the zeolite is set by the confinement set by the zeolite pores.[10] As a consequence, the entropy is calculated according to

$$S^{\mathrm{zeo}} = \frac{2}{3}\left(S^{\mathrm{gas}}_{\mathrm{trans}} + S^{\mathrm{gas}}_{\mathrm{rot}}\right) + S^{\mathrm{zeo}}_{\mathrm{vib}}. \tag{4}$$

Here, $S^{\mathrm{gas}}_{\mathrm{trans}}$ and $S^{\mathrm{gas}}_{\mathrm{rot}}$ are entropy contributions from the gas-phase translations and rotations of the molecule, and $S^{\mathrm{zeo}}_{\mathrm{vib}}$ is the entropy contribution from the vibrational modes of the molecule inside the zeolite.

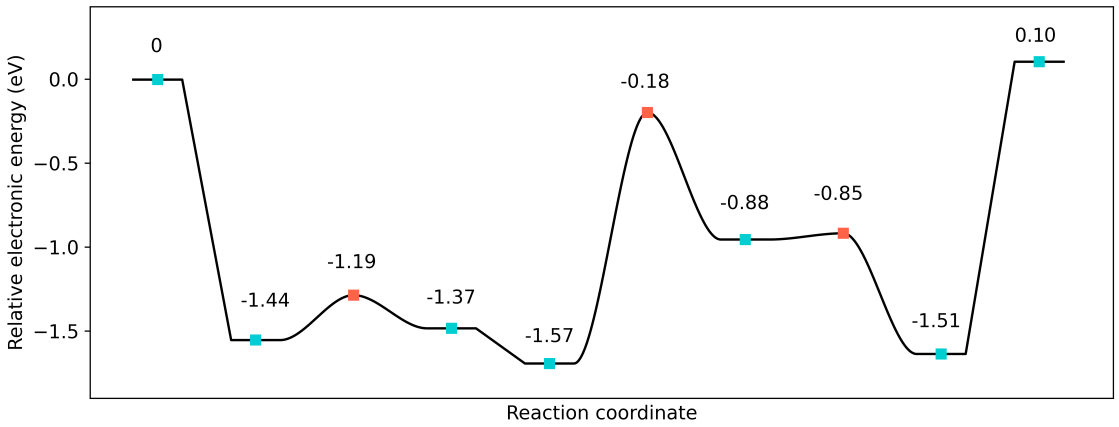

Figure S7: The total energy of the reaction landscape, as calculated from DFT. The structures associated with each step of the mechanism can be found in the main text, figure 3.

References

[1] Simone Creci, Anna Martinelli, Szilvia Vavra, Per-Anders Carlsson, and Magnus Skoglundh. Acidity as descriptor for methanol desorption in B-, Ga-and Ti-MFI zeotypes. *Catalysts*, 11(1):1–12, 2021.

[2] Christopher Sauer, Guido J. L. de Reijer, Andreas Schaefer, and Per-Anders Carlsson. Isomorphous Substitution of Gallium into MFI-Framework Zeolite Increases 2,5-Dimethylfuran to Aromatics Selectivity and Suppresses Catalyst Deactivation. *Topics in Catalysis*, 1:1–12, 12 2022.

[3] Xueting Wang, Adam A Arvidsson, Magdalena O Cichocka, Xiaodong Zou, Natalia M Martin, Johan Nilsson, Stefan Carlson, Johan Gustafson, Magnus Skoglundh, Anders Hellman, and Per-Anders Carlsson. Methanol Desorption from Cu-ZSM-5 Studied by in Situ Infrared Spectroscopy and First-Principles Calculations. *Journal of Physical Chemistry C*, 121(49):27389–27398, 2017.

[4] Simone Creci, Xueting Wang, Per-Anders Carlsson, and Magnus Skoglundh. Tuned Acidity for Catalytic Reactions: Synthesis and Characterization of Fe- and Al-MFI Zeotypes. *Topics in Catalysis*, 62(7-11):689–698, 8 2019.

[5] Simone Creci. *Tuned acidity in zeotypes: A descriptor to unravel the direct conversion of methane to methanol*. PhD thesis, Chalmers University of Technology, Gothenburg, 2020.

[6] Ch. Baerlocher and L.B. McCusker. Database of Zeolite Structures.

[7] H. van Koningsveld, J. C. Jansen, and H. van Bekkum. The monoclinic framework structure of zeolite H-ZSM-5. Comparison with the orthorhombic framework of as-synthesized ZSM-5. *Zeolites*, 10(4):235–242, 4 1990.

[8] Christopher Sauer, Anders Lorén, Andreas Schaefer, and Per-Anders Carlsson. On-Line Composition Analysis of Complex Hydrocarbon Streams by Time-Resolved Fourier Transform Infrared Spectroscopy and Ion–Molecule Reaction Mass Spectrometry. *Analytical Chemistry*, 93(39):13187–13195, 10 2021.

[9] Nan Yu Topsøe, Karsten Pedersen, and Eric G. Derouane. Infrared and temperature-programmed desorption study of the acidic properties of ZSM-5-type zeolites. *Journal of Catalysis*, 70(1):41–52, 7 1981.

[10] J. J. Mortensen, L. B. Hansen, and K. W. Jacobsen. Real-space grid implementation of the projector augmented wave method. *Physical Review B - Condensed Matter and Materials Physics*, 71(3):035109, 1 2005.

[11] J. Enkovaara, C. Rostgaard, J. J. Mortensen, J. Chen, M. Dułak, L. Ferrighi, J. Gavnholt, C. Glinsvad, V. Haikola, H. A. Hansen, H. H. Kristoffersen, M. Kuisma, A. H. Larsen, L. Lehtovaara, M. Ljungberg, O. Lopez-Acevedo, P. G. Moses, J. Ojanen, T. Olsen, V. Petzold, N. A. Romero, J. Stausholm-Møller, M. Strange, G. A. Tritsaris, M. Vanin, M. Walter, B. Hammer, H. Häkkinen, G. K.H. Madsen, R. M. Nieminen, J. K. Nørskov, M. Puska, T. T. Rantala, J. Schiøtz, K. S. Thygesen, and K. W. Jacobsen. Electronic structure calculations with GPAW: a real-space implementation of the projector augmented-wave method. *Journal of physics. Condensed matter : an Institute of Physics journal*, 22(25), 2010.

[12] P. E. Blöchl. Projector augmented-wave method. *Physical Review B*, 50(24):17953, 12 1994.

[13] M. Dion, H. Rydberg, E. Schröder, D. C. Langreth, and B. I. Lundqvist. Van der Waals density functional for general geometries. *Physical Review Letters*, 92(24):246401, 6 2004.

[14] Kristian Berland and Per Hyldgaard. Exchange functional that tests the robustness of the plasmon description of the van der Waals density functional. *Physical Review B - Condensed Matter and Materials Physics*, 89(3):035412, 1 2014.

[15] Ask Hjorth Larsen, Jens Jørgen Mortensen, Jakob Blomqvist, Ivano E. Castelli, Rune Christensen, Marcin Dułak, Jesper Friis, Michael N. Groves, Bjørk Hammer, Cory Hargus, Eric D. Hermes, Paul C. Jennings, Peter Bjerre Jensen, James Kermode, John R. Kitchin, Esben Leonhard Kolsbjerg, Joseph Kubal, Kristen Kaasbjerg, Steen Lysgaard, Jón Bergmann Maronsson, Tristan Maxson, Thomas Olsen, Lars Pastewka, Andrew Peterson, Carsten Rostgaard, Jakob Schiøtz, Ole Schütt, Mikkel Strange, Kristian S. Thygesen, Tejs Vegge, Lasse Vilhelmsen, Michael Walter, Zhenhua Zeng, and Karsten W. Jacobsen. The atomic simulation environment—a Python library for working with atoms. *Journal of Physics: Condensed Matter*, 29(27):273002, 6 2017.